Vortex ice pattern evolution in a kagome nanostructured superconductor

Xing-Hong Chen,[1] Xiu-De He,[1] An-Lei Zhang,[1] Victor V. Moshchalkov,[2] and Jun-Yi Ge[1,3,*]

[1]*Materials Genome Institute, Shanghai University, 200444 Shanghai, China*

[2]*Department of Physics and Astronomy, KU Leuven, Celestijnenlaan 200D, B–3001 Leuven, Belgium*

[3]*Physics Department, and Shanghai Key Laboratory of High Temperature Superconductors, Shanghai University, 200444 Shanghai, China*

(Received 23 May 2020; revised 24 July 2020; accepted 3 August 2020; published 21 August 2020)

The vortex ice system has been proposed as a promising platform to study the geometrical frustration and the emergent exotic phenomena, mainly because of the availability of tunable vortex-vortex interactions and the feasibility to manufacture a variety of nanoscale pinning potential geometries. In this paper, we designed and fabricated a kagome lattice of paired antidots with geometrical frustration. By changing the magnetic field to tune the number of interaction units, the vortex ice pattern formation and its evolution are revealed. We have found that only local topological charge order is formed at low magnetic fields, while the vortex pattern enters a disordered paramagnetic state with no long-range order of chirality or topological charge at relatively high magnetic fields. Instead of the expected half matching field in a vortex ice, the vertices fulfill the ice rule, reaching the maximum proportion at $0.7H_1$ due to the appearance of interstitial vortices. The correlation of vortex interaction also confirms such nontrivial matching field.

DOI: 10.1103/PhysRevB.102.054516

I. INTRODUCTION

Spin ice is a class of geometric frustrated magnetic materials that exhibit many interesting physical phenomena such as the low energy degeneracy [1,2], residual entropy [3–5], magnetic monopole excitations, and the Dirac strings [6–10]. However, experimental studies on spin ice materials have two unavoidable limitations. First, the material parameters (such as lattice constants) cannot be easily adjusted. Secondly, the limited approach to probe the individual spin in a large volume of spin ice material makes the study of magnetic excitations and the ground state rather inaccessible [11]. The two significant limitations in spin ice materials can both be circumvented by using the artificial spin ice (ASI) system [11–16]. Due to the development of the e-beam lithography, ferromagnetic islands have been introduced to explore the properties of frustrated systems [7,8,17–21]. The geometrical parameters of ASI systems (e.g., geometrical structure [22–24], array symmetry and periodicity [11,25], magnetic moment [26], etc.) can be tuned in many different ways. The single-domain ferromagnetic island in ASI can be fabricated to mimic the giant Ising spin [11,27–29], which can be directly imaged with, e.g., the magnetic force microscope [30] and x-ray magnetic circular dichroism [31]. In this way, it is possible to study the statistics of different magnetic states in the artificial spin ice (ASI) systems [16,32].

The ground state in ASI is essential to understand low energy degeneracy in ASI systems. However, the fairly weak dipole interactions can hardly lead to the long-range ordered ground state [25,26,33]. The number of elemental interaction units (FM islands) is fixed once an ASI structure is made [23]. As is known, vortices in type-II superconductors exhibit long-range, strong, electromagnetic interactions. When sitting at artificial pinning centers where superconductivity is locally suppressed, the vortex pattern is energetically favorable [34–36]. It is easy to tune the size of vortices and the vortex-vortex (V-V)/vortex-pinning interaction strength by altering the magnetic field and temperature. Moreover, the number of vortices can be easily controlled by changing the applied magnetic field, making the study of vortex pattern evolution possible. Therefore, the vortex system serves as a promising platform to study particle interactions on a potential-energy landscape with well-tuned geometries [37–39]. In artificial spin ice, due to the geometrical frustration, it is impossible to arrange all the magnetic moments in a way to minimize the interaction energy between every two moments (spins). The arrangement of the magnetic moments with the minimum energy has to follow the so-called ice rule: two-in/two-out. In our nanostructured superconductors, when replacing each magnetic moment with a paired antidot, it is also impossible to arrange all the vortices to minimize their interactions when only one antidot is occupied in each pair. For each vertex formed by three antidots (from three different pairs), the ice rule has to be fulfilled to minimize their interaction energy, i.e., two-occupied/one-free. This allows us to study the geometrical frustration in superconducting systems. The design of geometrical frustration using vortex matter (vortex ice) was first proposed in Ref. [40], where perfect ground state is expected to form at half matching field ($H = H_1/2$). Transport measurements also reveal nontrivial matching effects in such vortex-ice systems [41,42]. The filling rules of degenerate vortex states in a kagome lattice of elongated antidots are similar to the ice rules [37]. More recently, the square vortex ice state has been directly visualized by using a low-temperature scanning Hall probe microscope (SHPM) [43], revealing much

*junyi_ge@t.shu.edu.cn

more complex excitation states by changing the magnetic field. Very recently, the kagome vortex ice has been studied [44] by randomly imaging a few local vortex patterns; the authors show that the vortex ice state can be preserved with magnetic field up to $2H_1/3$ due to the appearance of interstitial vortices. Despite the stability of a vortex ice as a function of the lattice parameters, the intrinsic pairwise antidots interaction defined by lattice geometry and vortex interaction is crucial to understand the different ice state configurations. Also, the possible inner phase transition that might appear in the vortex ice system also needs to be revealed. However, the analysis of pairwise antidots interactions which needs a relatively large area for statistics has not been addressed yet.

Here we report the results of SHPM measurements on a nanostructured kagome lattice superconductor, which allows directly imaging a large area of vortex states and vertex configurations. By changing the magnetic field, we study in detail the formation and breakdown of a vortex ice state. We have found that both the proportion of ice pairs and ice rule vertices reach the maximum value at $0.7H_1$. The pairwise antidots interaction correlation as a function of magnetic field also attains the maximum at $0.7H_1$, thus confirming that the system minimizes the energy of pairwise antidot interactions at $0.7H_1$. No long-range ordered state has been observed in our sample. Our results suggest that the interstitial vortices play an important role in determining the vortex states in kagome vortex ice.

II. EXPERIMENTS

The studied nanostructured superconductor was fabricated by using the conventional electron-beam lithography technique. As shown in Fig. 1, the designed kagome lattice consists of adjacent pairs of antidots with the same center-to-center distance of 2 μm. In each pair, the antidot has the size of 0.6×0.6 μm^2 with the same center-to-center distance of 2 μm. In the kagome lattice, each vertex is composed of three antidot pairs, the interaction of which determines the vertex configurations. The superconducting film was a Pb film with the thickness of 60 nm, on top of which 10 nm Ge layer was deposited to protect the superconducting film from oxidation. Afterwards, the sample is covered by another layer of 35 nm thick Au, playing the role of the conducting layer for the approach of the Hall sensor via a scanning tunneling microscope tip [45]. For our nanostructured superconductor, the first matching field H_1 is calculated to be 2.57 Oe. The matching field corresponds to the situation that each antidot is occupied by one vortex. We define H_a as the applied external magnetic field. The vortex patterns froze at temperatures very close to Tc. Under the small magnetic field used in our sample, the frozen temperature is above 0.99 Tc. Even for a plain film with randomly distributed weak pinning centers, the vortex pattern freezes just below T_c [46]. So all SHPM images are acquired at 4.25 K with the Hall probe flying at 600 nm away from the sample surface.

III. RESULTS AND DISCUSSIONS

As shown in Fig. 1(c), the antidot pair presents two possible states with only one antidot being occupied (ice pair) and

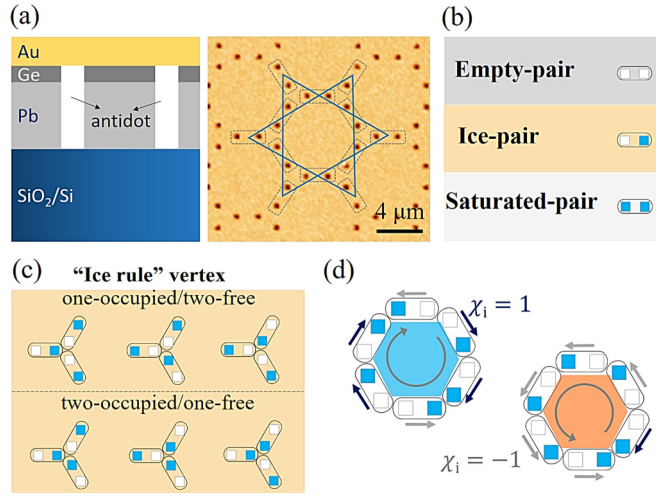

FIG. 1. (a) Schematic diagram (left panel) showing the side view of the studied nanostructured superconductor. Atomic-force microscope image (right panel) of the sample, where the kagome lattice of the paired antidots is indicated. (b) Various vortex occupation configurations for the paired antidots: empty pair with two free antidots, ice pair with only one antidot being occupied, and saturated pair with both antidots being occupied. (c) Six vertex configurations following the vortex-ice rule: two-occupied/one-free or one-occupied/two-free. (d) Following the way in Ref. [45], for each ice pair, a pseudospin is defined with the direction pointing toward the vortex. Six antidot pairs form a hexagon with the spin chirality defined by arrows ($\chi_i = 1$ clockwise, $\chi_i = -1$ counterclockwise). The hexagon is colored according to their net spin chirality: clockwise (blue), counterclockwise (orange).

can therefore be mapped into a spin system [40]. Nevertheless, there are two more possible vortex configurations for one antidot pair, which cannot be mapped into a spin ice system, namely, empty pairs without any antidots being occupied and saturated pairs with double occupation. Figure 1(c) presents six possible 'ice rule' vertex states formed by three ice pairs. Besides the vertices with one-in/two-out and two-in/one-out configurations, more intricate configurations can be formed, which are unique properties compared with artificial spin ice systems.

One advantage of the vortex ice system is that the number of vortices can be tuned by changing the external magnetic field. This allows the study of vortex ice pattern evolution with the number of interaction units, which is important to understand the emergent frustration-related phenomenon in ice systems. Figures 2(a)–2(k) show the evolution of vortex patterns under different magnetic fields as indicated in each image. The upper panels of Figs. 2(a)–2(k) are the experimental vortex ice configurations and the lower panels show the corresponding schematic diagrams, where the antidot positions are indicated as squares. The chirality of the hexagons is also indicated as defined in Fig. 1(d). The pinned and interstitial vortices are marked as blue squares and circles, respectively. We can see that not all the vortices are pinned even at magnetic field much smaller than half matching field. This is different from what was observed in a square lattice vortex ice, where all the vortices stay at antidot positions below first matching field. Here, the appearance of interstitial vortices can be attributed to

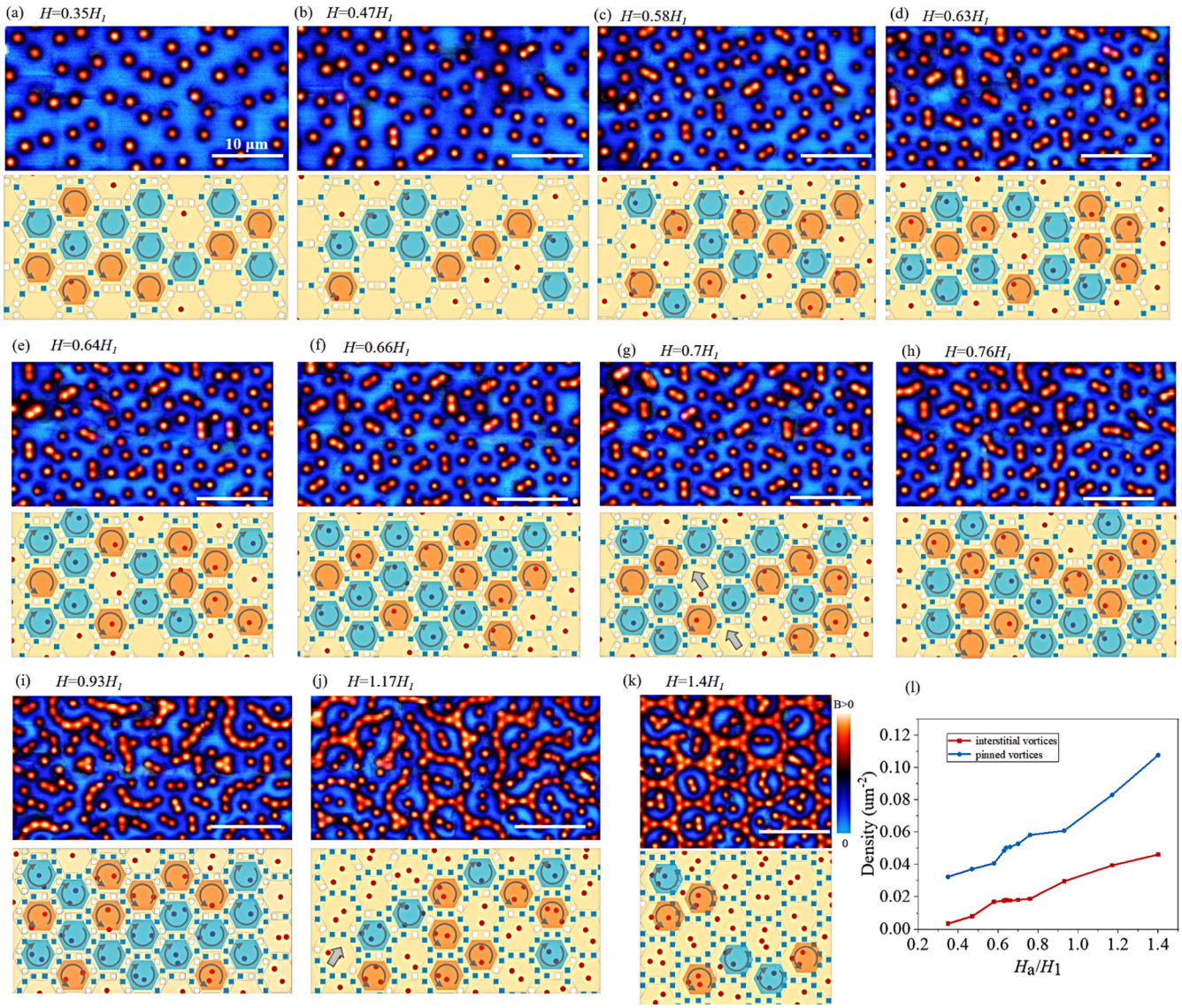

FIG. 2. (a)–(k) The observed vortex ice configurations (upper panels) and their schematic diagrams (lower panels) under various magnetic fields as indicated above each image. 10 μm for all the scale bars. (l) The density of interstitial and pinned vortices as a function of reduced magnetic field.

the relatively large plain area among antidots, where it is energetically favorable for vortices to stay away from the adjacent pinned vortices. With increasing the cooling magnetic field, the numbers of both interstitial and pinned vortices increase as shown in Fig. 2(l). At low fields, only ice pair and empty pairs are formed.

As an increase of the ice pairs, more and more vertices fulfill the vortex ice rule, i.e., one-occupied (free)/two-free (occupied), to minimize the total interaction energy. Such an ice rule leads to large degeneracy. At relatively small field [Fig. 2(a)], one-occupied/two-free vertex dominates. All the vortices are nearly homogeneously distributed in the sample. At relatively high magnetic field, the proportion of two-occupied/one-free vertices progressively increases and reaches maximum around $H = 0.7H_1$ [Fig. 2(g)]. This can be seen from the increased number of vortex dimers in Figs. 2(b)–2(g). However, no saturated pair is observed due to its high interaction energy. Besides the ice pair, we have found that, close to $0.5H_1$, there still exists a large number of empty pairs. This is different from what was expected for a vortex ice system, where a perfect ice state should form at half matching field [37,40,42] with equal number of one-occupied/two-free and two-occupied/one-free configurations. In our case, such a perfect ice state is observed at $H = 0.7H_1$ with the disappearance of the empty pairs [Fig. 2(g)]. This indicates that $H = 0.7H_1$ is the most equilibrium state for our studied kagome vortex ice. In our studied kagome lattice, besides the antidot, there exists another effective pinning potential which is the hexagon area surrounded by six pairs of antidots. As a result, the effective half matching field H* is increased from $0.5H_1$ to $0.7H_1$. This is also evidenced by the fact that, around $H = 0.7H_1$, the interstitial vortices are homogeneously distributed in the hexagons. The numerical constant 0.7 is not universal for all parameters considering the fact that, in a nanostructured superconductor, whether an antidot can be occupied depends on the pinning strength of the antidot and the vortex-vortex

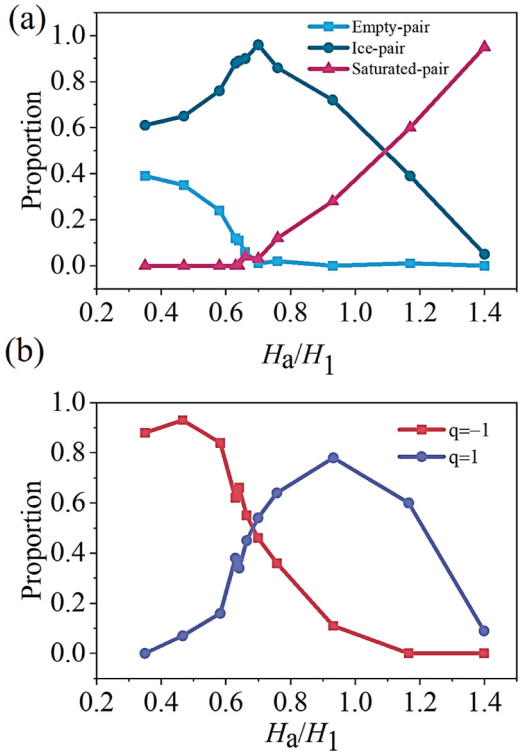

FIG. 3. Statistics of vortex ice states at different fields. (a) The proportion of different pair distributions [ice pairs (red circle), empty pairs (black square), and saturated pairs (cyan triangle)]. (b) The proportion of $q = 1$ and $q = -1$ vertices corresponding to the ice rule of 'two-occupied/one-free' and 'one-occupied/two-free,' respectively.

interactions. The vortex-vortex interaction strongly depends on the vortex-vortex distance (i.e., the antidot lattice constant). A detail simulation of kagome lattices with different lattice constants would even help to reveal the appearance and the evolution of the possible defects (e.g., the monopolelike excitations in spin ice). With increasing magnetic field above $0.7H_1$, more vortices start to occupy the antidots and the hexagons. Saturated pairs, with higher energy than ice pairs, start to appear. This is manifested by the vortex trimers as seen in Fig. 2(h). At further higher magnetic fields, fragments of vortex chains form as seen in Figs. 2(i)–2(j). Finally, around $H = 1.4H_1$ (effective first matching field), most of the pinning centers are occupied [Fig. 2(k)]. For the hexagons surrounded by six antidot pairs, we have also studied the spin chirality as defined in Fig. 1(d). It is seen from Figs. 2(a)–2(j) that, in our measured field range, no ordered state is observed. This might indicate that vertex configurations are in the paramagnetic state as observed in the colloid ice.

This vortex arrangements can generate degeneracy and a large configuration entropy. It is important to quantitatively analyze the vortex pattern evolution by looking at the proportion of various vortex states at different magnetic fields. The data extracted from Fig. 2 are summarized in Fig. 3(a). Starting from a fully vortex-free state, the vortex configuration experiences a rapid drop and rise in the empty-pair and ice-pair populations, respectively, while no saturated pair is formed. At $H = 0.35H_1$, nearly 60% of paired antidots is occupied by one vortex (ice pair). Then, with the appearance

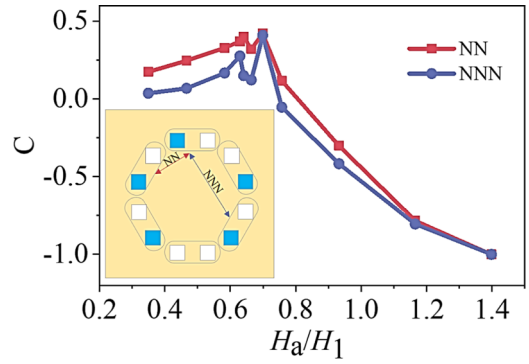

FIG. 4. The defined correlations as a function of magnetic field. The inset shows the definitions of the nearest neighbor pairs (NN) and the next nearest neighbor pairs (NNN).

of interstitial vortices, the change of empty pair/ice pair is slowing down. The proportion of ice pair (empty pair) reaches maximum (minimum) at $H = 0.7H_1$, above which the proportion of saturated pair starts becoming nonzero. Both saturated pair and ice pair follow linear dependences with magnetic field up to $1.4H_1$.

The distribution of topological charge q provides important information about the inner phases in both ASI and colloid ice systems [47]. Here, in our kagome lattice, $q = n_o - n_f$ is defined as the difference between the number of occupied (n_o) and free (n_f) antidots of each vertex. The proportion of different topological charges as a function of magnetic field is shown in Fig. 3(b). It is seen that, around $H = 0.4H_1$ [see Figs. 2(a) and 2(b)] and $H = 0.9H_1$, local charge ordering (LCO) states are formed with most of the vertices obeying $q = -1$ and $q = 1$, respectively. Such LCO states are unique compared with the colloid ice system where $q = 1$ is impossible due to the fact that the number of colloid particles are fixed. Therefore, the numbers of $q = 1$ and $q = -1$ must equalize. From Fig. 3(a), we can see that the state with equal $q = 1$ and $q = -1$ is observed at $H = 0.7H_1$, further confirming this effective half matching field.

To further understand the frustration in this system, we calculate the intrinsic pairwise correlations [32] between the three types of antidot pairs. To set up a proper correlation function, we consider the interactions between distinct types of neighboring antidot pairs. The closest pairing is defined as the nearest neighbor (NN), while the next nearest neighbor pairing is named NNN (see Fig. 4 inset). We define a correlation C such that $C = +1$ when two antidot pairs are aligned to minimize the vortex-vortex (v-v) interaction energy. We thus define $C = +1$ when the two pairs are both empty pair or the two ice pairs that the direction of the occupied antidot by vortex to the empty antidot (A-A direction) is clockwise or counterclockwise. We define $C = 0$ when a pair is an empty pair or the nearest antidots of the two pairs are both free. We also define $C = -1$ when a pair is a saturated pair or the nearest antidots of the two pairs are both occupied. In this way, the bigger the average value of C, the smaller v-v interaction energy of the kagome lattice.

The calculated correlation values at different magnetic fields are shown in Fig. 4. We find that C_{NN} and C_{NNN} have the same trend that the both values increase first and then

decrease with magnetic field. The correlation values reach the maximum at $0.7H_1$, where the proportions of ice-pair and ice vertices dominate. Therefore, we can confirm that the energetic favorable state is realized at $0.7H_1$. Moreover, we find that the existence of only short-range order and icelike correlations in the system is similar to the behavior of the spin ice materials. It is also analogous to the artificial kagome spin ice where the ice rule is strictly obeyed with no instance of non-ice-rule vertices. In our sample, the presence of interstitial vortices plays an important role in stabilizing the ice patterns. It would be interesting to further study such nontrivial matching effect by transport measurement.

IV. CONCLUSION

In conclusion, the vortex ice pattern formation and breakdown in a superconducting film with a kagome lattice of paired antidots has been directly visualized by using the SHPM. We find that, due to the presence of interstitial vortices, the number of vertices fulfilling the ice rule increases until $0.7\,H_1$ which is different from other vortex ice lattices. In all the measured field range, no long-range topological charge order is observed. The system remains in the paramagnetic disordered state. Our results show the controllability of vortex ice systems which is important to unveil the fundamental nature of geometrical frustration in various ice systems.

ACKNOWLEDGMENTS

We thank J. Van de Vondel and V. S. Zharinov for the help with making the sample. The study was supported by the National Key Research and Development Program of China (Grant No. 2018YFA0704300), National Natural Science Foundation of China (Grant No. 11804217), the Methusalem funding by the Flemish government, and the Flemish Science Foundation (FWO). J.-Y.G. also thanks the support by the Program for Professor of Special Appointment (Eastern Scholar) at Shanghai Institutions of Higher Learning.

[1] Y. Perrin, B. Canals, and N. Rougemaille, Nature (London) **540**, 410 (2016).
[2] G.-W. Chern, P. Mellado, and O. Tchernyshyov, Phys. Rev. Lett. **106**, 207202 (2011).
[3] A. F. Hebard and A. T. Fiory, in *Future Trends in Superconductive Electronics*, edited by B. S. Deaver, Jr, C. M. Falco, J. H. Harris, and S. A. Wolf, AIP Conf. Proc. No. 44 (AIP, New York, 1978), p. 465.
[4] G. C. Lau, R. S. Freitas, B. G. Ueland, B. D. Muegge, E. L. Duncan, P. Schiffer, and R. J. Cava, Nat. Phys. **2**, 249 (2006).
[5] D. Pomaranski, L. R. Yaraskavitch, S. Meng, K. A. Ross, H. M. L. Noad, H. A. Dabkowska, B. D. Gaulin, and J. B. Kycia, Nat. Phys. **9**, 353 (2013).
[6] S. Ladak, D. E. Read, G. K. Perkins, L. F. Cohen, and W. R. Branford, Nat. Phys. **6**, 359 (2010).
[7] O. Romero-Isart, C. Navau, A. Sanchez, P. Zoller, and J. I. Cirac, Phys. Rev. Lett. **111**, 145304 (2013).
[8] W. Branford, S. Ladak, D. E. Read, K. Zeissler, and L. F. Cohen, Science **335**, 1597 (2012).
[9] A. Farhan, P. M. Derlet, A. Kleibert, A. Balan, R. V. Chopdekar, M. Wyss, L. Anghinolfi, F. Nolting, and L. J. Heyderman, Nat. Phys. **9**, 375 (2013).
[10] I. Gilbert, Y. Lao, I. Carrasquillo, L. O'Brien, J. D. Watts, M. Manno, C. Leighton, A. Scholl, C. Nisoli, and P. Schiffer, Nat. Phys. **12**, 162 (2016).
[11] R. F. Wang, C. Nisoli, R. S. Freitas, J. Li, W. McConville, B. J. Cooley, M. S. Lund, N. Samarth, C. Leighton, V. H. Crespi, and P. Schiffer, Nature (London) **439**, 303 (2006).
[12] C. Nisoli, R. Moessner, and P. Schiffer, Rev. Mod. Phys. **85**, 1473 (2013).
[13] Y. L. Wang, Z. L. Xiao, A. Snezhko, J. Xu, L. E. Ocola, R. Divan, J. E. Pearson, G. W. Crabtree, and W.-K. Kwok, Science **352**, 962 (2016).
[14] C. Marrows, Nat. Phys. **9**, 324 (2013).
[15] U. B. Arnalds, A. Farhan, R. V. Chopdekar, V. Kapaklis, A. Balan, E. Th. Papaioannou, M. Ahlberg, F. Nolting, L. J. Heyderman, and B. Hjörvarsson, Appl. Phys. Lett. **101**, 112404 (2012).
[16] V. Kapaklis, U. B. Arnalds, A. Farhan, R. V. Chopdekar, A. Balan, A. Scholl, L. J. Heyderman, and B. Hjörvarsson, Nat. Nanotechnol. **9**, 514 (2014).
[17] S. A. Daunheimer, O. Petrova, O. Tchernyshyov, and J. Cumings, Phys. Rev. Lett. **107**, 167201 (2011).
[18] P. E. Lammert, X. Ke, J. Li, C. Nisoli, D. M. Garand, V. H. Crespi, and P. Schiffer, Nat. Phys. **6**, 786 (2010).
[19] L. J. Heyderman, Nat. Nanotechnol. **8**, 705 (2013).
[20] M. J. Morrison, T. R. Nelson, and C. Nisoli, New J. Phys. **15**, 045009 (2013).
[21] I. Gilbert, G.-W. Chern, S. Zhang, L. O'Brien, B. Fore, C. Nisoli, and P. Schiffer, Nat. Phys. **10**, 670 (2014).
[22] S. Zhang, I. Gilbert, C. Nisoli, G.-W. Chern, M. J. Erickson, L. O'Brien, C. Leighton, P. E. Lammert, V. H. Crespi, and P. Schiffer, Nature (London) **500**, 553 (2013).
[23] V. S. Bhat, J. Sklenar, B. Farmer, J. Woods, J. T. Hastings, S. J. Lee, J. B. Ketterson, and L. E. De Long, Phys. Rev. Lett. **111**, 077201 (2013).
[24] A. Farhan, A. Scholl, C. F. Petersen, L. Anghinolfi, C. Wuth, S. Dhuey, R. V. Chopdekar, P. Mellado, M. J. Alava, and S. van Dijken, Nat. Commun. **7**, 12635 (2016).
[25] J. Li, X. Ke, S. Zhang, D. Garand, C. Nisoli, P. Lammert, V. H. Crespi, and P. Schiffer, Phys. Rev. B **81**, 092406 (2010).
[26] Z. Budrikis, J. P. Morgan, J. Akerman, A. Stein, P. Politi, S. Langridge, C. H. Marrows, and R. L. Stamps, Phys. Rev. Lett. **109**, 037203 (2012).
[27] L. Anghinolfi, H. Luetkens, J. Perron, M. G. Flokstra, O. Sendetskyi, A. Suter, T. Prokscha, P. M. Derlet, S. L. Lee, and L. J. Heyderman, Nat. Commun. **6**, 8278 (2015).
[28] C. Nisoli, J. Li, X. Ke, D. Garand, P. Schiffer, and V. H. Crespi, Phys. Rev. Lett. **105**, 047205 (2010).
[29] S. Zhang, J. Li, I. Gilbert, J. Bartell, M. J. Erickson, Y. Pan, P. E. Lammert, C. Nisoli, K. K. Kohli, R. Misra, V. H. Crespi, N. Samarth, C. Leighton, and P. Schiffer, Phys. Rev. Lett. **109**, 087201 (2012).

[30] J. M. Porro, A. Bedoya-Pinto, A. Berger, and P. Vavassori, New J. Phys. **15**, 055012 (2013).
[31] A. Farhan, P. M. Derlet, A. Kleibert, A. Balan, R. V. Chopdekar, M. Wyss, J. Perron, A. Scholl, F. Nolting, and L. J. Heyderman, Phys. Rev. Lett. **111**, 057204 (2013).
[32] Y. Qi, T. Brintlinger, and J. Cumings, Phys. Rev. B **77**, 094418 (2008).
[33] X. Ke, J. Li, C. Nisoli, P. E. Lammert, W. McConville, R. F. Wang, V. H. Crespi, and P. Schiffer, Phys. Rev. Lett. **101**, 037205 (2008).
[34] D. Davidović, S. Kumar, D. H. Reich, J. Siegel, S. B. Field, R. C. Tiberio, and R. Hey, and K. Ploog, Phys. Rev. B **55**, 6518 (1997).
[35] J.-Y. Ge, V. N. Gladilin, C. Xue, J. Tempere, J. T. Devreese, J. Van de Vondel, Y. Zhou, and V. V. Moshchalkov, Phys. Rev. B **93**, 224502 (2016).
[36] C. C. de Souza Silva, J. Van de Vondel, M. Morelle, and V. V. Moshchalkov, Nature (London) **440**, 651 (2006).
[37] C. Xue, J.-Y. Ge, A. He, V. S. Zharinov, V. V. Moshchalkov, Y. H. Zhou, A. V. Silhanek, and J. Van de Vondel, Phys. Rev. B **96**, 024510 (2017).
[38] G. Karapetrov, J. Fedor, M. Iavarone, D. Rosenmann, and W. K. Kwok, Phys. Rev. Lett. **95**, 167002 (2005).
[39] D. Ray, C. J. Olson Reichhardt, B. Janko, and C. Reichhardt, Phys. Rev. Lett. **110**, 267001 (2013).
[40] A. Libál, C. J. Olson Reichhardt, and C. Reichhardt, Phys. Rev. Lett. **102**, 237004 (2009).
[41] J. Trastoy, M. Malnou, C. Ulysse, R. Bernard, N. Bergeal, G. Faini, J. Lesueur, J. Briatico, and J. E. Villegas, Nat. Nanotechnol. **9**, 710 (2014).
[42] M. L. Latimer, G. R. Berdiyorov, Z. L. Xiao, F. M. Peeters, and W. K. Kwok, Phys. Rev. Lett. **111**, 067001 (2013).
[43] J.-Y. Ge, V. N. Gladilin, J. Tempere, V. S. Zharinov, J. Van de Vondel, J. T. Devreese, and V. V. Moshchalkov, Phys. Rev. B **96**, 134515 (2017).
[44] C. Xue, J.-Y. Ge, A. He, V. S. Zharinov, V. V. Moshchalkov, Y. H. Zhou, A. V. Silhanek, and J. Van de Vondel, Phys. Rev. B **97**, 134506 (2018).
[45] J.-Y. Ge, J. Gutierrez, V. N. Gladilin, J. T. Devreese, and V. V. Moshchalkov, Nat. Commun. **6**, 6573 (2015).
[46] A. V. Silhanek, M. V. Milosevic, R. B. G. Kramer, G. R. Berdiyorov, J. Van de Vondel, R. F. Luccas, T. Puig, F. M. Peeters, and V. V. Moshchalkov, Phys. Rev. Lett. **104**, 017001 (2010).
[47] A. Libál, C. Nisoli, C. J. O. Reichhardt, and C. Reichhardt, Phys. Rev. Lett. **120**, 027204 (2018).